How Are Different Neural Networks Related to Consciousness?

Pengmin Qin, PhD,[1,2,3] Xuehai Wu, PhD,[4] Zirui Huang, PhD,[2]
Niall W. Duncan, PhD,[1,2,3,5] Weijun Tang, PhD,[6] Annemarie Wolff, PhD,[1]
Jin Hu, PhD,[4] Liang Gao, PhD,[4] Yi Jin, PhD,[4] Xing Wu, PhD,[4]
Jianfeng Zhang, MS,[5] Lu Lu, MS,[6] Chunping Wu, MS,[6] Xiaoying Qu, MS,[6]
Ying Mao, PhD,[4] Xuchu Weng, PhD,[5] Jun Zhang, PhD,[7] and
Georg Northoff, PhD[1,2,3,5,8]

Objective: We aimed to investigate the roles of different resting-state networks in predicting both the actual level of consciousness and its recovery in brain injury patients.

Methods: We investigated resting-state functional connectivity within different networks in patients with varying levels of consciousness: unresponsive wakefulness syndrome (UWS; n = 56), minimally conscious state (MCS; n = 29), and patients with brain lesions but full consciousness (BL; n = 48). Considering the actual level of consciousness, we compared the strength of network connectivity among the patient groups. We then checked the presence of connections between specific regions in individual patients and calculated the frequency of this in the different patient groups. Considering the recovery of consciousness, we split the UWS group into 2 subgroups according to recovery: those who emerged from UWS (UWS-E) and those who remained in UWS (UWS-R). The above analyses were repeated on these 2 subgroups.

Results: Functional connectivity strength in salience network (SN), especially connectivity between the supragenual anterior cingulate cortex (SACC) and left anterior insula (LAI), was reduced in the unconscious state (UWS) compared to the conscious state (MCS and BL). Moreover, at the individual level, SACC-LAI connectivity was more present in MCS than in UWS. Default-mode network (DMN) connectivity strength, especially between the posterior cingulate cortex (PCC) and left lateral parietal cortex (LLPC), was reduced in UWS-R compared with UWS-E. Furthermore, PCC-LLPC connectivity was more present in UWS-E than in UWS-R.

Interpretation: Our findings show that SN (SACC-LAI) connectivity correlates with behavioral signs of consciousness, whereas DMN (PCC-LLPC) connectivity instead predicts recovery of consciousness.

ANN NEUROL 2015;78:594–605

Consciousness is a multifaceted phenomenon whose neural correlates remain the subject of intense investigation. Recent proposals have suggested that the brain's intrinsic activity, often measured during the so-called resting state, may be an important process underlying consciousness.[1,2] Such resting-state activity can be separated into different neural networks defined by correlated activity patterns between the constituent subregions. In addition to their anatomy, the different neural networks may also be distinguished in functional terms. For instance, the default-mode network (DMN) is thought to be related to internally oriented thought,[3] whereas the executive-control network (ECN) may be related to externally guided awareness.[4] A third network—the salience

network (SN)—has been linked with the conscious perception of stimuli.[5,6]

Given these links between the 3 resting-state networks and differing aspects of consciousness, questions arise as to their exact roles in constituting or supporting consciousness. More specifically, these links highlight the potential clinical importance of particular networks in conditions where consciousness is impaired.[7] To study this question, network activity and its effect on altered states of consciousness, such as unresponsive wakefulness syndrome (UWS; formally unknown as vegetative state), minimally conscious state (MCS), and anesthesia, have been investigated.[8–11] The results of these studies have been inconsistent, however, and the studies have not explicitly investigated how the networks may be differentially related to consciousness.[12]

In UWS and MCS patients, the main focus of research has been the DMN.[12,13] Some studies have shown that functional connectivity within the DMN is altered in such patients,[14,15] but others have found this network to be intact in coma patients who regained consciousness,[16] in UWS patients,[17] and in conscious but sedated humans.[18] In addition, the DMN appears to be intact in both anesthetized humans[19] and anesthetized monkeys.[20] These apparently contradictory results leave unclear the exact relationship between the DMN and consciousness. Less work has focused upon the SN and ECN in altered states of consciousness. The SN and ECN showed reduced functional connectivity during drug-induced unconsciousness,[4] but any differences in these networks in disorders of consciousness (DOC) patients (UWS and MCS) remain to be fully investigated.[21]

The overall aim of our study was thus to use resting-state functional magnetic resonance imaging (fMRI) to investigate each of the 3 aforementioned networks (DMN, ECN, and SN) in UWS and MCS. We sought, first, to establish in which network activity properties best distinguish levels of consciousness. In addition, we also aimed to investigate which network could be used to predict consciousness recovery. To these ends, we utilized a group of healthy participants (n = 52) to independently identify the different networks. The delineated networks were then applied to patients with either UWS (n = 56) or MCS (n = 29), and the functional connectivity within them was calculated. These functional connectivity values were analyzed in line with the study aims to identify the networks associated with consciousness level and with clinical recovery. As the effect of tissue damage itself, as distinguished from functional changes per se, represents a potential confound for such analyses, we included a group of patients with brain lesions but full consciousness (BL; n = 48) as a control group along with the UWS and MCS patients.

Subjects and Methods

Participants

The study included 52 healthy controls, 56 UWS patients, 29 MCS patients, and 48 patients with BL (see Table 1 and Supplementary Tables 1–3 for participant details). None of the healthy participants had a history of neurological or psychiatric disorders, nor were they taking any kind of medication. The UWS and MCS patients were assessed using the Coma Recovery Scale–Revised (CRS-R)[22] before fMRI scanning (T0). The Glasgow Outcome Scale (GOS) was carried out at least 3 months after the scan session (T1). For some aspects of the analysis, the UWS group was divided into 2 subgroups based on their GOS scores at T1. These subgroups were those who emerged from UWS (UWS-E) and those who remained in UWS (UWS-R). UWS patients with a GOS score of <3 were classified as UWS-R, whereas patients with a score ≥ 3 were classified as UWS-E. The BL patients were recruited as a control group.

The CRS-R was performed following the administration and scoring guidelines.[22] The CRS-R was translated into Chinese by 3 authors (P.Q., Z.H., and Xu.Wu.). Xu.Wu., an experienced neurosurgeon, performed the CRS-R and GOS assessments while blinded to the fMRI data analysis. DOC patients were recruited from Huashan Hospital in Shanghai and its affiliated rehabilitation centers. BL patients were recruited from both the inpatient and outpatient neurosurgical clinics at Huashan Hospital. Patients with metal implants or abnormal temperature were excluded. Patients who required sedation or anesthesia were also excluded, as were those who required a ventilator. For the UWS patients, the follow-up assessment at T1 (ie, 3 months postscanning) was carried out at Huashan Hospital. Informed written consent was obtained from the healthy participants and from the patients' legal representatives. The study was approved by the Ethics Committee of Shanghai Huashan Hospital, Fudan University, Shanghai, China.

fMRI Data Acquisition

All magnetic resonance images were acquired on the same Siemens (Erlangen, Germany) 3T scanner. For the healthy controls, functional images were acquired using a T2*-weighted echo-planar imaging sequence (repetition time [TR] = 2,000 milliseconds, echo time [TE] = 35 milliseconds, $\theta = 90°$, field of view [FOV] = 256 × 256mm, matrix = 64 × 64, slice thickness = 4mm, gap = 0mm). Each volume had 33 axial slices, covering the whole brain. Two hundred volumes were acquired during rest. The same functional parameters were used for 92 of the 133 UWS, MCS, and BL patients. In the remaining 41 patients, the same scanner was used but with different scan parameters, as follows. In 10 of them, the parameters were: 33 slices, TR = 2,000 milliseconds, TE = 30 milliseconds, $\theta = 90°$, FOV = 210 × 210mm, matrix = 64 × 64, slice thickness = 5mm, gap = 0mm, 180 volumes; in 31 of them, the parameters were: 33 slices, TR = 2,000 milliseconds, TE = 30 milliseconds, $\theta = 90°$, FOV = 210 × 210mm, matrix = 64 × 64, slice thickness = 4mm, gap = 0mm, 200 volumes. This

TABLE 1. Demographic and Clinical Information for Participant Groups

Group	Number	Mean Age, yr (SD)	Female, No.	Days since Injury (SD)	Residual Brain Volume, mm³ (SD)	Traumatic Injury, No.
Healthy participants	52	35 (9)	15	n/a	1,171,747 (45,023.8)	n/a
BL	48	42 (15)	11	149 (146)	1,092,191 (96,810.7)	44
MCS	29	44 (13)	6	119 (162)	1,049,592 (133,641.6)	24
UWS	56	41 (14)	14	96 (74)	1,054,256 (124,029.6)	41
UWS-R	30	45 (14)	9	130 (114)	1,024,419 (119,821.5)	20
UWS-E	23	38 (12)	5	68 (57)	1,102,173 (110,919.9)	19

Diagnosis was made according to the Coma Recovery Scale–Revised. See Supplementary Tables (1–3) for detailed information. The UWS group was further divided into 2 subgroups (UWS-E and UWS-R). UWS-R consists of those patients who remained in a UWS at least 3 months after their initial assessment, whereas UWS-E consists of the patients who had emerged from UWS at 3 months. There were 3 UWS patients without follow-up information. There was no difference in age or sex between the 3 patient groups (BL, MCS, and UWS), nor any difference in the time since injury. The residual brain volume was defined using a partial volume threshold of 0.8 for the gray and white matter segmentations. There was no difference of brain volume between the 3 patient groups. For the 2 UWS subgroups (UWS-E and UWS-R), there was no difference in age, gender, or time since injury. There was, however, a significant difference in brain volume ($p = 0.018$).
BL = brain lesion with full consciousness; MCS = minimally conscious state; n/a = not applicable; SD = standard deviation; UWS = unresponsive wakefulness syndrome.

difference in acquisition parameters was taken into account in the ultimate statistical analyses. To further ensure that the different acquisition parameters were not influencing our results, we repeated the analysis using only the 92 participants who had the same parameters. The same results were obtained. A high-resolution T1-weighted anatomical image was acquired for all participants for functional image registration and localization (TR = 2,300 milliseconds, TE = 2.98 milliseconds, matrix = 256 × 256, slice thickness = 1mm). All participants (healthy controls and patients) were instructed by the same researcher (W.T.) to take a comfortable supine position, relax, close their eyes, and not to concentrate on anything in particular during the scanning.[17,21,23] All participants wore earplugs to minimize the noise of the scanner.

Data Preprocessing

Anatomical images were segmented into gray matter, white matter, and cerebrospinal fluid (CSF), using the FAST tool from the FSL software package (http://www.fmrib.ox.ac.uk/fsl/). Functional images were processed using the AFNI software package.[24] After discarding the first 2 volumes, functional images then underwent a preprocessing procedure that included: slice-timing correction, 2- and 3-dimensional head motion corrections, masking for the removal of the skull, and spatial smoothing using a 8mm full width at half maximum kernel.[21] Time series were then normalized by computing the ratio of the signal in each voxel at each time point to the mean across all time points, and then multiplying by 100. The 6 estimated head motion parameters and the mean time series from the white matter and the CSF—where these regions were defined using partial volume thresholds of 0.99 for each tissue type—were considered as noise covariates and were regressed out from the data.[25] The data were band-pass filtered, reserving signals between 0.01 and 0.08Hz.[26] Note that in our analysis we did not remove the global mean. To ensure that this did not influence out results, we repeated the analysis including global mean removal and found no difference.

Head Motion Correction

The issue of motion artifacts was addressed rigorously, as minor group differences in motion have been shown to cause artificial group differences.[27–29] Motion was quantified as the Euclidean distance calculated from the 6 rigid-body motion parameters for 2 consecutive time points (AFNI, 1d_tool.py). Any instance of movement > 0.5mm was considered as excessive motion, for which the respective volume as well as the immediately preceding and subsequent volumes were removed.[30] To obtain reliable results, participants with <3 minutes worth of data remaining were excluded.[31] This resulted in the exclusion of 3 UWS patients, 1 MCS patient, and 1 BL patient. Among the patient groups, the number of remaining volumes were compared. BL patients (190 ± 16; mean ± standard deviation) had more volumes remaining than UWS (182 ± 24.6) and MCS (177 ± 25.6) patients. To confirm that our results were not confounded by these differing data lengths, we shortened the BL data to match those of the UWS and MCS patients and repeated the statistical analysis. No difference in the results was seen.

Defining Regions of Interest

Structural and functional images from the healthy control group were transformed into Montreal Neurological Institute (MNI) standard space ($2 \times 2 \times 2mm^3$ resolution). We used these healthy control data to define the 3 target resting-state networks: SN,[6,32] DMN,[33] and ECN.[32,34] To define these networks, we first selected seed regions according to the AFNI

Brain Region	Location	MNI Coordinates		
		X	Y	Z
Salience network				
SACC	M	−1	20	28
LAI	L	−42	14	0
RAI	R	40	12	0
LTHAL	L	−12	−16	4
RTHAL	R	14	−20	8
Default-mode network				
PCC	M	0	−46	20
MPFC	M	0	56	−6
LLPC	L	−42	−68	38
RLPC	R	50	−60	36
RTP	R	58	−2	−22
Executive-control network				
LDLPFC	L	−36	52	10
RDLPFC	R	34	46	20
LIPL	L	−40	−56	44
RIPL	R	46	−52	44
PCUN	M	4	−42	44

TABLE 2. Coordinates of Regions of Interest in MNI Standard Space

L = left; LAI = left anterior insula; LDLPFC = left dorsal lateral prefrontal cortex; LIPL = left inferior parietal lobe; LLPC = left lateral parietal cortex; LTHAL = left thalamus; M = medial; MNI = Montreal Neurological Institute; MPFC = medial prefrontal cortex; PCC = posterior cingulate cortex; PCUN = precuneus; R = right; RAI = right anterior insula; RDLPFC = right dorsal lateral prefrontal cortex; RIPL = right inferior parietal lobe; RLPC = right lateral parietal cortex; RTHAL = right thalamus; RTP = right temporal pole; SACC = supragenual anterior cingulate cortex.

thresholding these mean images at $Z > 0.3095$ ($r > 0.30$) with a cluster extent threshold of 100 voxels. The 5 largest clusters in each of the network images were identified, and spherical regions of interest (ROIs) with a radius of 10mm were placed at the peak coordinate within each (see Table 2 for the coordinates of each ROI).[36]

These ROIs were then warped onto the non-normalized functional images for the individual patients.[37,38] The procedure to do this was as follows. Functional images were individually coregistered with structural images; structural images were then normalized to MNI standard space; the inverse of the structural to MNI and functional to structural transformations were combined to give individual MNI to functional transforms; and, finally, these transformations were applied to the ROIs to align them with the functional images. The location of each ROI was visually checked for each patient (see Fig 1 for sample ROI localizations). As some patients have enlarged ventricles, the CSF segmentation image calculated previously was used to mask any ventricle voxels from within the warped ROIs.[39] Any ROIs with <10 voxels following alignment to functional space and masking for ventricle voxels were excluded.[17] This resulted in the exclusion of 32 ROIs in total (5 in SN, 17 in DMN, and 10 in ECN). Full details of the excluded ROIs, along with the number of voxels constituting each included ROI, can be found in Supplementary Table 4. The number of voxels remaining in each ROI for each patient was included as a covariate in the subsequent data analyses.

Functional Connectivity

For each network (SN, DMN, and ECN), the mean time series was extracted from each subregion ROI. The Pearson correlation coefficient between the time series of each pair of ROIs was calculated as a measure of functional connectivity. Fisher Z transformation was used to transform the correlation r values to normally distributed Z values. The average Z value across all pairs of ROIs within each network was then computed.

Statistical Analysis

In a first step, we sought to identify in which networks as a whole functional connectivity could distinguish unconscious (UWS) and conscious (MCS and BL) states. To do this, the mean functional connectivity across all ROIs for each network (ie, the mean network connectivity) was compared between the 3 groups through 1-way analyses of variance (ANOVAs). Note that prior to these group comparisons, functional connectivity Z values were corrected for patient age,[14] the different acquisition parameters,[40] mean head motion, the volume of the relevant ROIs, the length of time since brain injury, and the total brain volume, through linear regression. Post hoc t tests were then used to determine which specific groups showed differences in each network. One-tailed tests were used for the post hoc testing, as previous studies showed reduced functional connectivity in unconscious, as compared to conscious, states. A false discovery rate (FDR) correction including all 3 networks was performed to account for the combined total of 9 post hoc tests.

anatomical template (TT_desai_dk_mpm).[35] For the SN, the seed region was the supragenual anterior cingulate cortex (SACC); for the DMN, the seed was the posterior cingulate cortex (PCC); and for the ECN, it was the right dorsal lateral prefrontal cortex. Next, voxelwise resting-state functional connectivity maps for the healthy controls were computed for each of the 3 seed regions. To do this, the mean blood oxygenation level–dependent time series in each specific seed region was correlated with the time series in every other voxel using Pearson linear correlation. The resulting r values were converted to normally distributed Z values using Fisher Z transform. Group functional connectivity maps for each of the 3 networks were then created by averaging the individual Z value images and

TABLE 3. Functional Connectivity between Each Pair of Regions in the 3 Networks for UWS, MCS, and BL (Z Values; Mean ± Standard Error)

SN	SACC-LAI	SACC-RAI	SACC-LTHAL	SACC-RTHAL	LAI-RTHAL	LAI-LTHAL	LAI-RAI	LTHAL-RAI	LTHAL-RTHAL	RAI-RTHAL
UWS	0.17 (0.04)[a,b]	0.18 (0.03)	0.08 (0.04)[b]	0.07 (0.04)[b]	0.19 (0.04)	0.21 (0.04)	0.30 (0.05)	0.16 (0.04)	0.64 (0.05)[a]	0.28 (0.05)
MCS	0.43 (0.07)	0.28 (0.07)	0.16 (0.06)	0.17 (0.05)	0.27 (0.05)	0.28 (0.05)	0.45 (0.08)	0.18 (0.05)	0.84 (0.05)	0.27 (0.06)
BL	0.41 (0.05)	0.38 (0.04)	0.22 (0.04)	0.25 (0.04)	0.31 (0.04)	0.29 (0.03)	0.56 (0.06)	0.21 (0.04)	0.78 (0.03)	0.31 (0.04)
DMN	PCC-LLPC	PCC-RLPC	PCC-MPFC	PCC-RTP	LLPC-RTP	LLPC-MPFC	LLPC-RLPC	MPFC-RLPC	MPFC-RTP	RLPC-RTP
UWS	0.43 (0.04)[b]	0.39 (0.05)	0.30 (0.05)	0.17 (0.04)[b]	0.09 (0.04)[b]	0.24 (0.04)	0.25 (0.04)[b]	0.32 (0.04)	0.21 (0.05)	0.34 (0.05)
MCS	0.56 (0.05)	0.52 (0.06)	0.29 (0.05)	0.27 (0.06)	0.25 (0.09)	0.23 (0.05)	0.37 (0.09)	0.21 (0.05)	0.18 (0.08)	0.45 (0.06)
BL	0.70 (0.04)	0.54 (0.06)	0.51 (0.06)	0.41 (0.04)	0.38 (0.04)	0.37 (0.04)	0.56 (0.06)	0.38 (0.04)	0.33 (0.04)	0.43 (0.04)
ECN	PCUN-LIPL	PCUN-RIPL	PCUN-LDLPFC	PCUN-RDLPFC	LIPL-RDLPFC	LIPL-LDLPFC	LIPL-RIPL	LDLPFC-RIPL	LDLPFC-RDLPFC	RIPL-RDLPFC
UWS	0.27 (0.05)	0.39 (0.05)	0.15 (0.05)	0.22 (0.04)	0.14 (0.04)	0.35 (0.05)	0.25 (0.05)	0.08 (0.05)	0.30 (0.05)	0.38 (0.05)
MCS	0.36 (0.07)	0.51 (0.07)	0.33 (0.06)	0.23 (0.06)	0.11 (0.07)	0.26 (0.07)	0.36 (0.09)	0.24 (0.08)	0.38 (0.10)	0.32 (0.06)
BL	0.35 (0.05)	0.41 (0.04)	0.30 (0.05)	0.21 (0.04)	0.24 (0.04)	0.35 (0.05)	0.47 (0.06)	0.24 (0.04)	0.48 (0.05)	0.38 (0.05)

[a]Represents a significant difference between UWS and MCS.
[b]Represents a significant difference between UWS and BL. The significance threshold is $p < 0.05$ (false discovery rate corrected).
BL = brain lesions but full consciousness; DMN = default-mode network; ECN = executive-control network; LAI = left anterior insula; LDLPFC = left dorsal lateral prefrontal cortex; LIPL = left inferior parietal lobe; LLPC = left lateral parietal cortex; LTHAL = left thalamus; MCS = minimally conscious state; MPFC = medial prefrontal cortex; PCC = posterior cingulate cortex; PCUN = precuneus; RAI = right anterior insula; RDLPFC = right dorsal lateral prefrontal cortex; RIPL = right inferior parietal lobe; RLPC = right lateral parietal cortex; RTHAL = right thalamus; RTP = right temporal pole; SACC = supragenual anterior cingulate cortex; SN = salience network; UWS = unresponsive wakefulness syndrome.
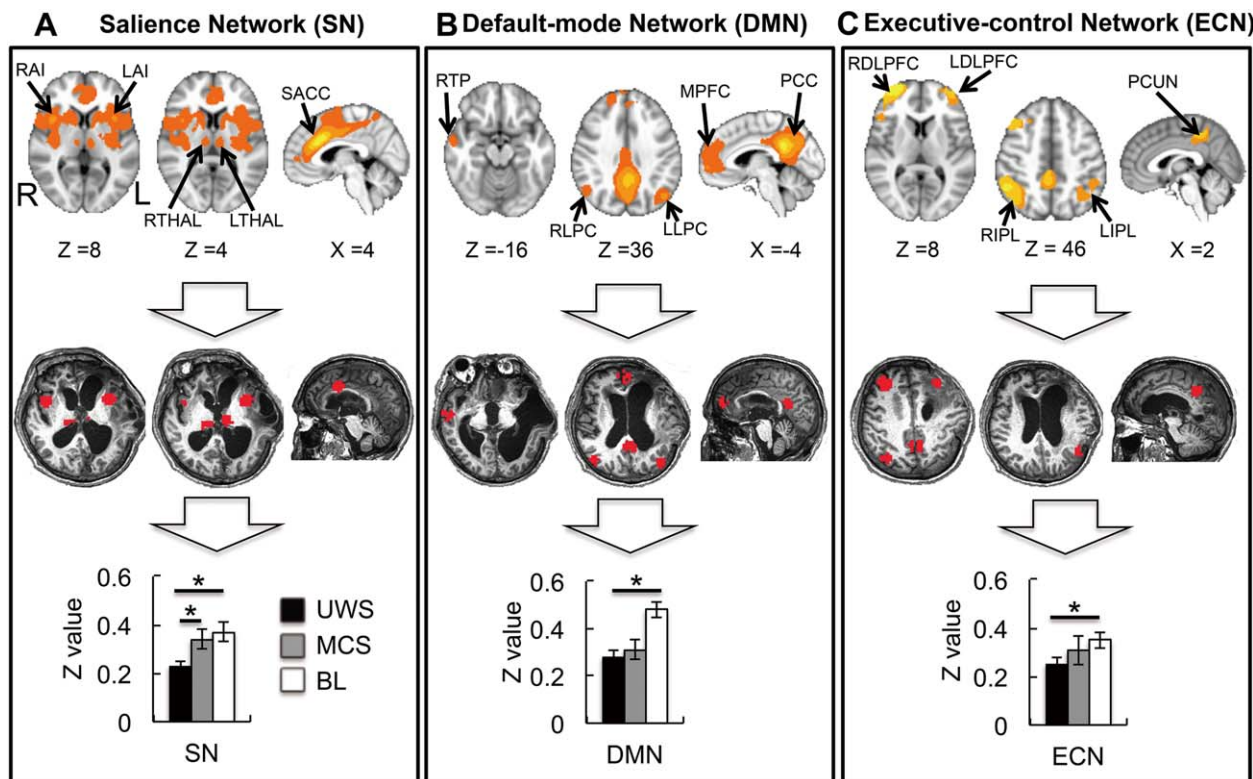
FIGURE 1: Functional connectivity in (A) the salience network (supragenual anterior cingulate cortex as seed region), (B) the default-mode network (posterior cingulate cortex as seed region), and (C) the executive-control network (right dorsal lateral prefrontal cortex as seed region) in healthy controls. For each, the top panel shows functional connectivity maps on a standard brain template; the middle panel shows the corresponding regions of interest on a single patient's anatomical image (Patient 14); and the bottom panel shows the comparison of functional connectivity between the UWS, MCS, and BL groups (mean ± standard error) at the network level (ie, mean functional connectivity within each network). *$p < 0.05$, corrected. BL = brain lesions but full consciousness; LAI = left anterior insula; LDLPFC = left dorsal lateral prefrontal cortex; LIPL = left inferior parietal lobe; LLPC = left lateral parietal cortex; LTHAL = left thalamus; MCS = minimally conscious state; MPFC = medial prefrontal cortex; PCC = posterior cingulate cortex; PCUN = precuneus; RAI = right anterior insula; RDLPFC = right dorsal lateral prefrontal cortex; RIPL = right inferior parietal lobe; RLPC = right lateral parietal cortex; RTHAL = right thalamus; RTP = right temporal pole; SACC = supragenual anterior cingulate cortex; UWS = unresponsive wakefulness syndrome. [Color figure can be viewed in the online issue, which is available at www.annalsofneurology.org.]

To further specify which regions are most able to distinguish conscious from unconscious states, we then carried out a similar analysis using the corrected values for functional connectivity between individual pairs of ROIs within each of the 3 networks (ANOVAs followed by post hoc t tests). With 3 networks, 3 patient groups, and 5 regions within each network, a total of 90 post hoc tests were carried out. FDR correction was used to control for the multiple comparison problem across all 90.

Having identified which networks and pairs of regions could distinguish between conscious and unconscious states, we then examined the possibility of using functional connectivity within the identified regions to differentiate UWS and MCS patients. For each region-pair functional connectivity that showed a significant difference in connectivity strength between UWS and MCS at the group level, a threshold of $r \geq 0.3$ was used to determine whether connectivity was present in each patient.[41,42] The frequency of connectivity being present was then compared between UWS and MCS (chi-square test). In addition, receiver operating characteristic (ROC) curves were plotted for the relevant region-pair functional connectivity values. For these, a cor-

rect classification of MCS was counted as a true positive. The area under the ROC curve was taken as a measure of diagnostic accuracy. The maximum Youden index along the given curve (defined as J = sensitivity + specificity − 1) was taken as the cutoff point for classification accuracy.[43]

For the UWS-R and UWS-E groups, we repeated the same analysis to test the relationship between functional connectivity and the recovery of consciousness. Chi-square tests assessed the difference in the ratio of presence between UWS-R and UWS-E ($p < 0.05$). For ROC analysis, the area under the ROC curve as a measure of the accuracy of prediction of the recovery of consciousness.

Finally, we sought to establish the specificity of the relationship between a particular region-pair's functional connectivity and either the differentiation of behavioral signs of consciousness or the recovery of consciousness. To do this, the ROC curves for the different region-pairs tested were compared in each of these comparisons (UWS vs MCS = behavioral signs of consciousness; UWS-E vs UWS-R = recovery of consciousness).

TABLE 4. Functional Connectivity between Each Pair of Regions in the 3 Networks for UWS-R and UWS-E (Z Values; Mean ± Standard Error)

SN	SACC-LAI	SACC-RAI	SACC-LTHAL	SACC-RTHAL	LAI-RTHAL	LAI-LTHAL	LAI-RAI	LTHAL-RAI	LTHAL-RTHAL	RAI-RTHAL
UWS-R	0.13 (0.05)	0.18 (0.03)	0.09 (0.05)	0.08 (0.05)	0.16 (0.04)	0.20 (0.04)	0.26 (0.07)	0.13 (0.06)	0.56 (0.06)	0.26 (0.06)
UWS-E	0.22 (0.05)	0.28 (0.07)	0.05 (0.06)	0.03 (0.06)	0.28 (0.08)	0.27 (0.07)	0.33 (0.08)	0.27 (0.06)	0.74 (0.08)	0.34 (0.07)
DMN	PCC-LLPC	PCC-RLPC	PCC-MPFC	PCC-RTP	LLPC-RTP	LLPC-MPFC	LLPC-RLPC	MPFC-RLPC	MPFC-RTP	RLPC-RTP
UWS-R	0.29 (0.06)[a]	0.32 (0.07)	0.23 (0.06)	0.14 (0.06)	0.03 (0.06)	0.22 (0.05)	0.19 (0.06)	0.32 (0.05)	0.20 (0.05)	0.27 (0.07)
UWS-E	0.61 (0.07)	0.48 (0.07)	0.38 (0.07)	0.23 (0.06)	0.18 (0.05)	0.26 (0.07)	0.32 (0.06)	0.33 (0.07)	0.22 (0.07)	0.41 (0.06)
ECN	PCUN-LIPL	PCUN-RIPL	PCUN-LDLPFC	PCUN-RDLPFC	LIPL-RDLPFC	LIPL-LDLPFC	LIPL-RIPL	LDLPFC-RIPL	LDLPFC-RDLPFC	RIPL-RDLPFC
UWS-R	0.15 (0.06)	0.30 (0.08)	0.04 (0.06)	0.19 (0.05)	0.12 (0.03)	0.35 (0.08)	0.37 (0.07)	0.03 (0.08)	0.22 (0.08)	0.37 (0.07)
UWS-E	0.46 (0.08)	0.54 (0.07)	0.27 (0.07)	0.26 (0.06)	0.15 (0.03)	0.35 (0.07)	0.33 (0.07)	0.13 (0.08)	0.36 (0.07)	0.26 (0.06)

[a]Represents a significant difference between UWS-R and UWS-E. The significance threshold is $p < 0.05$ (false discovery rate corrected).
DMN = default-mode network; ECN = executive-control network; LAI = left anterior insula; LDLPFC = left dorsal lateral prefrontal cortex; LIPL = left inferior parietal lobe; LLPC = left lateral parietal cortex; LTHAL = left thalamus; MPFC = medial prefrontal cortex; PCC = posterior cingulate cortex; PCUN = precuneus; RAI = right anterior insula; RDLPFC = right dorsal lateral prefrontal cortex; RIPL = right inferior parietal lobe; RLPC = right lateral parietal cortex; RTHAL = right thalamus; RTP = right temporal pole; SACC = supragenual anterior cingulate cortex; SN = salience network; UWS = unresponsive wakefulness syndrome; UWS-E = emerged from UWS; UWS-R = remained in UWS.

Results

Functional Connectivity and Level of Consciousness

The networks of interest—DMN, ECN, and SN—were identified in the independent healthy control group (see Fig 1). The connectivity Z values in the 3 networks were then compared in the patient groups.

The ANOVA for the SN showed a significant group effect ($F = 6.89$, $p = 0.003$, corrected). Post hoc tests identified a reduction in connectivity strength in the UWS group, as compared to the MCS ($p = 0.01$, corrected) and BL groups ($p < 0.01$, corrected). There was no significant difference between the MCS and BL groups (see Fig 1). A significant group effect was also seen in the DMN ($F = 8.49$, $p < 0.01$, corrected). Post hoc tests showed that DMN connectivity was reduced in UWS when compared to BL ($p < 0.01$, corrected). There was no significant difference between UWS and MCS, nor between MCS and BL. Finally, there was no group effect in the ECN ($F = 2.56$, $p = 0.08$, corrected), although the post hoc tests did show a significant difference between UWS and BL ($p = 0.03$, corrected). There was no difference between UWS and MCS, nor between MCS and BL in the ECN. The SN is thus the only network that shows a difference in functional connectivity between conscious (MCS, BL) and unconscious (UWS) patients.

For connectivity between pairs of regions within each network, consistent with the results at the network level, only the functional connectivity strength between the SACC and left anterior insula (LAI) within the SN was significantly reduced in UWS compared to MCS ($p = 0.01$, corrected) and BL ($p = 0.02$, corrected). No other connectivity pairs showed a difference between UWS and MCS (Table 3).

As the group analysis showed that SACC-LAI connectivity was significantly reduced in UWS compared to MCS, we tested the difference in the frequency of the presence of SACC-LAI connectivity ($r \geq 0.3$) between UWS and MCS. The results showed that a SACC-LAI connection was more likely to be present in MCS than in UWS (chi-square = 9.16, $p = 0.002$; Fig 2B). An ROC analysis showed that the area under the ROC curve was 0.74 and was significantly related to behavioral signs of consciousness ($p = 0.001$). The cutoff threshold according to the Youden index was $r = 0.38$; the accuracy was 78.9%, with 65.2% sensitivity and 84.9% specificity (see Fig 2C).

Functional Connectivity and Recovery of Consciousness

To test which network was associated with an improvement in level of consciousness after at least 3 months, we
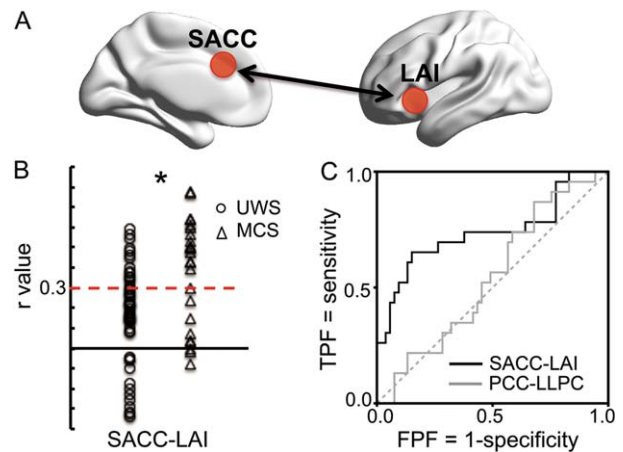

FIGURE 2: (A) Schemata of the functional connectivity between supragenual anterior cingulate cortex (SACC) and left anterior insula (LAI). (B) Individual SACC-LAI functional connectivity values for unresponsive wakefulness syndrome (UWS; n = 53) and minimally conscious state (MCS; n = 24) patients. The broken line represents $r = 0.3$. The presence of SACC-LAI connectivity ($r \geq 0.3$) was significantly correlated with consciousness level (chi-square = 9.16, $p = 0.002$). (C) Receiver operating characteristic plots for the prediction of behavioral signs of consciousness by SACC-LAI and posterior cingulate cortex (PCC)–left lateral parietal cortex (LLPC) connectivity. True positive fraction (TPF) = sensitivity to MCS; false positive fraction (FPF) = 1 − specificity to MCS. [Color figure can be viewed in the online issue, which is available at www.annalsofneurology.org.]

compared connectivity Z values between UWS-R and UWS-E groups in the 3 networks. The ANOVA for the SN showed no significant difference between UWS-R and UWS-E, meaning that the SN did not show any predictive effect for therapeutic recovery (Fig 3). Unlike the SN, functional connectivity in the DMN did predict the recovery of consciousness ($p = 0.01$, corrected). Finally, there was no significant difference in the ECN.

Consistent with the results at the network level, functional connectivity between the PCC and left lateral parietal cortex (LLPC; within the DMN) was significantly reduced in UWS-R compared to UWS-E ($p = 0.02$, corrected). No other pairs of regions showed a significant connectivity reduction in UWS-R compared to UWS-E (Table 4).

Considering that PCC-LLPC connectivity was significantly reduced in UWS-R compared to UWS-E, we tested the difference in the frequency of connectivity presence ($r \geq 0.3$) between UWS-R and UWS-E subjects. The results showed that PCC-LLPC connectivity was significantly more present in UWS-E than in UWS-R (chi-square = 8.64, $p = 0.003$; Fig 4B). An ROC analysis showed that the area under the ROC curve was 0.76, and significantly related to the recovery of consciousness ($p = 0.002$). According to the Youden index, the cutoff
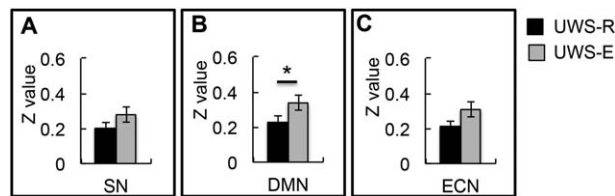
FIGURE 3: Functional connectivity in (A) the salience network (SN), (B) the default-mode network (DMN), and (C) the executive-control network (ECN). For each, bars show the comparison of functional connectivity strength between those who remained in unresponsive wakefulness syndrome (UWS) at T1 (UWS-R) and those who had emerged from UWS at T1 (UWS-E; mean ± standard error) at the network level (ie, the mean functional connectivity strength within each network). *$p < 0.05$ corrected.

threshold was $r = 0.37$; the accuracy was 74%, with 81% sensitivity and 69% specificity (see Fig 4C).

Specificity of the Relationship between Functional Connectivity and Behavioral Signs of Consciousness/Recovery of Consciousness

To test the specificity of the relationship between the SN (SACC-LAI) and behavioral signs of consciousness, we compared the ROC curve of SACC-LAI connectivity and prediction of consciousness level (ie, UWS vs MCS classification) with the ROC curve for the same classification using PCC-LLPC connectivity. A significant difference between the areas under the curve for these was observed ($p = 0.04$; see Fig 2C). Similarly, to test the specificity of the relationship between the DMN (PCC-LLPC) and the recovery of consciousness, the same comparison was done using ROC curves for the classification of UWS-R and UWS-E. Again, a significant difference between the areas under the curve for PCC-LLPC and SACC-LAI connectivity was seen ($p = 0.05$; see Fig 4C).

Discussion

A large sample of patients with UWS or MCS was used to investigate which resting-state networks are associated with different levels of consciousness. A group of patients with brain lesions but full consciousness were also studied to control for the effect of tissue damage. Among the 3 networks studied (the DMN, ECN, and SN), only connectivity within the SN could be used to reliably distinguish between conscious (MCS, BL) and unconscious (UWS) states. In particular, connectivity between the SACC and LAI allowed a reliable distinction. In addition, connectivity between the SACC and LAI was more present in MCS than UWS. Considering whether activity in particular networks could be used to predict clinical outcomes 3 months postscanning, it was found that connectivity within the DMN was lower in those who showed no improvement (UWS-R), as compared to those

who improved their level of consciousness (UWS-E). Furthermore, PCC-LLPC functional connectivity was more present in UWS-E than UWS-R. Finally, ROC curve analyses showed that the relationships with either the behavioral signs of consciousness or the recovery of consciousness were specific to SACC-LAI and PCC-LLPC connectivity, respectively. In summary, the SN and DMN showed distinguishable relationships with the behavioral signs or recovery of consciousness.

Salience Network and Consciousness

Recent investigations have demonstrated changes in resting-state networks in altered states of consciousness such as anesthesia[4,44] and UWS patients.[14,21] The current study also found reduced functional connectivity in these networks in altered states of consciousness, corroborating these prior findings. Our results extend existing work by demonstrating that only resting-state connectivity in the SN—and not the DMN or ECN—can be used to distinguish between conscious (MCS and BL) and unconscious (UWS) states.

Previous studies in both healthy participants and neurological patients have suggested a particular role for
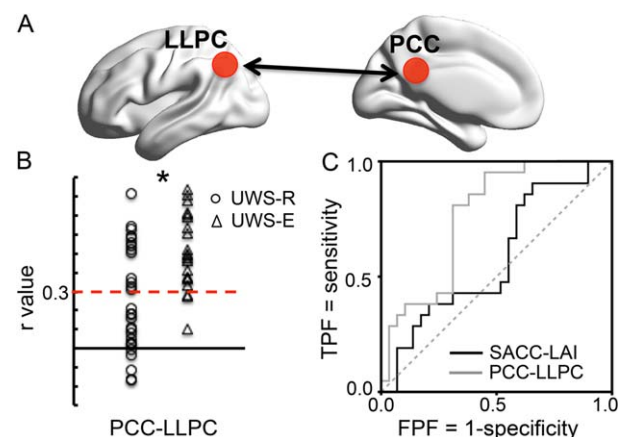

FIGURE 4: (A) Schemata of the functional connectivity between posterior cingulate cortex (PCC) and left lateral parietal cortex (LLPC). (B) Individual PCC-LLPC functional connectivity values for patients who remained in unresponsive wakefulness syndrome (UWS) at T1 (UWS-R; n = 29) and those who had emerged from UWS at T1 (UWS-E; n = 21) patients. (Note that, although there were 53 UWS patients after removing 3 patients with too much head motion from the total 56 patients, 3 of those lacked Glasgow Outcome Scale scores at T1 and were not included in this particular analysis.) The broken line represents $r = 0.3$. The presence of PCC-LLPC connectivity ($r \geq 0.3$) was significantly correlated with recovery of consciousness (chi-square = 8.64, *$p = 0.003$). (C) Receiver operating characteristic (ROC) plots for the prediction of the recovery of consciousness by supragenual anterior cingulate cortex (SACC)–left anterior insula (LAI) and PCC-LLPC connectivity. True positive fraction (TPF) = sensitivity to recovery of consciousness (UWS-E); false positive fraction (FPF) = 1 − specificity to UWS-E. [Color figure can be viewed in the online issue, which is available at www.annalsofneurology.org.]

the SACC in consciousness.[45–47] Moreover, our recent studies demonstrated that stimulus-induced activity in the SACC (in response to hearing the subject's own name or autobiographical statements) correlate with the level of consciousness in UWS patients.[30,37] Our present findings extend these results by showing that SACC resting-state activity, independent of stimulus-induced activity, is itself correlated with behavioral signs of consciousness. Additionally, the current results are consistent with recent findings in anesthesia where the source of altered electroencephalographic alpha band activity at the frontal electrodes during unconsciousness could be localized to the SACC.[48] Similarly, research in healthy participants suggests that neural activity in the SN is closely related to conscious perception.[45–47,49] Finally, it may be noted that the SN has been associated with the autonomic nervous system, and in particular with sympathetic outflow.[32,50] The correlation between SN functional connectivity and consciousness level may thus be partly mediated by the interaction between this system, the autonomic nervous system, and overall arousal levels. This remains speculative at present, however.

DMN and Recovery of Consciousness

The DMN shows higher activity during the resting state than during attention-demanding tasks.[51] As such, the DMN has been suggested to be involved in "mind-wandering"[52] and "self-referential processing."[34] Considering this link to specifically internally oriented processing, the DMN has therefore been thought to be involved in consciousness.[53] For this reason, prior studies on patients with DOC have mainly focused on the DMN.[7,21]

Such studies have indicated that DMN functional connectivity in patients with DOC is reduced in comparison to healthy controls.[14,15] This is consistent with our current results, where connectivity in the DMN is reduced in UWS as compared to BL patients. However, other studies have shown persistent DMN connectivity in UWS,[17] light sleep,[54] anesthesia in humans[19] and monkeys,[20] and acute coma patients.[16] Importantly, the latter coma study showed that the 2 patients with maintained DMN connectivity subsequently regained consciousness, whereas the other 11 coma patients without DMN connectivity did not.[16] These results led to a hypothesis that DMN connectivity may be necessary for consciousness to occur, but does not itself account for the level of consciousness.[55] Our current results showed that UWS-E patients have stronger functional connectivity (and a higher frequency of individual presence) in the DMN (PCC-LLPC) than UWS-R patients. This provides support for such a hypothesis.

ECN and Level of Consciousness

A previous study has shown altered ECN connectivity in patients with disorders of conscious when compared to healthy controls.[21] However, according to the current results, ECN connectivity showed no direct relationship with the level of consciousness, as documented by the absence of any differences between UWS/vegetative state and MCS. This is further supported by the absence of any significant difference in ECN functional connectivity between UWS-R and UWS-E. This leaves unclear the exact role of the ECN in constituting the level of consciousness, a question that may be investigated in detail in the future.

Clinical Implications

The results show that SN connectivity (SACC-LAI) may differentiate patients in MCS from patients in UWS, whereas DMN connectivity (PCC-LLPC) may differentiate those who recover consciousness after 3 months from those who do not (UWS-E/UWS-R). The accuracy of these predictions is not yet sufficient for direct translation to the clinic but are extremely promising. The accuracy values are similar to those of a recent fluorodeoxyglucose positron emission tomography (FDG-PET) study of vegetative state patients where global glucose metabolism was used for diagnosis (although note that this study did not report specificity or sensitivity values).[56] Our fMRI results are notable in this context, as FDG-PET has previously been suggested to be superior for the diagnosis of the level of consciousness, yet our results provide a degree of accuracy similar to that modality.[11] Furthermore, our fMRI results allowed the discrimination of different networks that were associated with different aspects of the clinical picture (ie, behavioral signs of consciousness and recovery of consciousness). They thus provide clear targets for future studies to develop directly applicable diagnostic and prognostic markers for DOC.

Methodological Limitations

Care must be taken when attempting to differentiate neuronal effects associated with the loss of consciousness from those related to brain lesions. To control for the effects of gross brain lesions, which may have a confounding impact on functional connectivity independent of the level of consciousness, our study included a control group of patients with brain lesions but full consciousness. However, the inclusion of the BL group is only relevant to the effects of large-scale brain damage and may not control for highly localized lesions (eg, subdural hemorrhage) or for generalized damage (eg, diffuse axonal injury), factors that may be relevant to DOC patient outcomes.[12] Additionally, considering the probability that an injured brain should be

considered a "new normal" rather than a merely deficient or "abnormal" system, the BL group may provide a more suitable control than healthy participants for comparing different networks between different patient groups.[10] Finally, in this analysis the GOS was used at T1 to classify UWS patients as either UWS-E or UWS-R. The CRS-R may, however, provide a more accurate measure of outcomes, and so we would recommend the use of this scale in conjunction with the GOS in future studies.

Conclusions

We investigated resting-state networks in a unique sample of patients with MCS, UWS, and BL. Unlike the DMN and ECN, resting-state functional connectivity in the SN, particularly SACC-LAI connectivity, was able to distinguish between conscious and unconscious states. Although DMN connectivity could not be used to distinguish between conscious and unconscious states, connectivity in the DMN, especially PCC-LLPC, was related to the recovery of consciousness. Our findings contribute to a better understanding of the distinct roles of different neural networks in constituting the level of consciousness in general. They also have important implications for imaging-based clinical diagnosis and prognosis in patients with DOC.

Authorship

P.Q., G.N., and Xu.Wu. designed the study. Z.H., Ji.Z., Xu.We., Y.M., and W.T. acquired imaging data. P.Q. and N.W.D. preprocessed imaging data. P.Q. did statistical analysis. J.H., Y.J., X.W., L.G., Ju.Z., C.W., X.Q., and L.L. recruited patients. P.Q., X.W., N.W.D., G.N., and A.W. wrote the report. All authors contributed to the subsequent drafts and approved the final version. P.Q. and Xu.Wu contributed equally to this work.

Potential Conflicts of Interest

Nothing to report.

References

1. Shulman RG, Hyder F, Rothman DL. Baseline brain energy supports the state of consciousness. Proc Natl Acad Sci U S A 2009; 106:11096–11101.

2. Northoff G. Unlocking the brain. Volume II: Consciousness. Oxford, UK: Oxford University Press, 2014.

3. Vanhaudenhuyse A, Demertzi A, Schabus M, et al. Two distinct neuronal networks mediate the awareness of environment and of self. J Cogn Neurosci 2011;23:570–578.

4. Boveroux P, Vanhaudenhuyse A, Bruno MA, et al. Breakdown of within- and between-network resting state functional magnetic resonance imaging connectivity during propofol-induced loss of consciousness. Anesthesiology 2010;113:1038–1053.

5. Boly M, Balteau E, Schnakers C, et al. Baseline brain activity fluctuations predict somatosensory perception in humans. Proc Natl Acad Sci U S A 2007;104:12187–12192.

6. Sadaghiani S, Scheeringa R, Lehongre K, et al. Intrinsic connectivity networks, alpha oscillations, and tonic alertness: a simultaneous electroencephalography/functional magnetic resonance imaging study. J Neurosci 2010;30:10243–10250.

7. Heine L, Soddu A, Gomez F, et al. Resting state networks and consciousness: alterations of multiple resting state network connectivity in physiological, pharmacological, and pathological consciousness States. Front Psychol 2012;3:295.

8. Giacino JT, Fins JJ, Laureys S, Schiff ND. Disorders of consciousness after acquired brain injury: the state of the science. Nat Rev Neurol 2014;10:99–114.

9. Casali AG, Gosseries O, Rosanova M, et al. A theoretically based index of consciousness independent of sensory processing and behavior. Sci Transl Med 2013;5:198ra05.

10. Di Perri C, Bastianello S, Bartsch AJ, et al. Limbic hyperconnectivity in the vegetative state. Neurology 2013;81:1417–1424.

11. Stender J, Gosseries O, Bruno MA, et al. Diagnostic precision of PET imaging and functional MRI in disorders of consciousness: a clinical validation study. Lancet 2014;384:514–522.

12. Di Perri C, Heine L, Amico E, et al. Technology-based assessment in patients with disorders of consciousness. Ann Ist Super Sanita 2014;50:209–220.

13. Crone JS, Schurz M, Holler Y, et al. Impaired consciousness is linked to changes in effective connectivity of the posterior cingulate cortex within the default mode network. Neuroimage 2015;110:101–109.

14. Vanhaudenhuyse A, Noirhomme Q, Tshibanda LJ, et al. Default network connectivity reflects the level of consciousness in non-communicative brain-damaged patients. Brain 2010;133(pt 1):161–171.

15. Cauda F, Micon BM, Sacco K, et al. Disrupted intrinsic functional connectivity in the vegetative state. J Neurol Neurosurg Psychiatry 2009;80:429–431.

16. Norton L, Hutchison RM, Young GB, et al. Disruptions of functional connectivity in the default mode network of comatose patients. Neurology 2012;78:175–181.

17. Boly M, Tshibanda L, Vanhaudenhuyse A, et al. Functional connectivity in the default network during resting state is preserved in a vegetative but not in a brain dead patient. Hum Brain Mapp 2009;30:2393–2400.

18. Greicius MD, Kiviniemi V, Tervonen O, et al. Persistent default-mode network connectivity during light sedation. Hum Brain Mapp 2008;29:839–847.

19. Martuzzi R, Ramani R, Qiu M, et al. Functional connectivity and alterations in baseline brain state in humans. Neuroimage 2010; 49:823–834.

20. Vincent JL, Patel GH, Fox MD, et al. Intrinsic functional architecture in the anaesthetized monkey brain. Nature 2007;447:83–86.

21. Demertzi A, Gomez F, Crone JS, et al. Multiple fMRI system-level baseline connectivity is disrupted in patients with consciousness alterations. Cortex 2014;52:35–46.

22. Giacino JT, Kalmar K, Whyte J. The JFK Coma Recovery Scale-Revised: measurement characteristics and diagnostic utility. Arch Phys Med Rehabil 2004;85:2020–2029.

23. Voss HU, Heier LA, Schiff ND. Multimodal imaging of recovery of functional networks associated with reversal of paradoxical herniation after cranioplasty. Clin Imaging 2011;35:253–258.

24. Cox RW. AFNI: software for analysis and visualization of functional magnetic resonance neuroimages. Comput Biomed Res 1996;29: 162–173.

25. Saad ZS, Gotts SJ, Murphy K, et al. Trouble at rest: how correlation patterns and group differences become distorted after global signal regression. Brain Connect 2012;2:25–32.

26. Yan C, Liu D, He Y, et al. Spontaneous brain activity in the default mode network is sensitive to different resting-state conditions with limited cognitive load. PloS One 2009;4:e5743.

27. Power JD, Barnes KA, Snyder AZ, et al. Spurious but systematic correlations in functional connectivity MRI networks arise from subject motion. Neuroimage 2012;59:2142–2154.

28. Van Dijk KR, Sabuncu MR, Buckner RL. The influence of head motion on intrinsic functional connectivity MRI. Neuroimage 2012; 59:431–438.

29. Satterthwaite TD, Elliott MA, Gerraty RT, et al. An improved framework for confound regression and filtering for control of motion artifact in the preprocessing of resting-state functional connectivity data. Neuroimage 2013;64:240–256.

30. Huang Z, Dai R, Wu X, et al. The self and its resting state in consciousness: an investigation of the vegetative state. Hum Brain Mapp 2013;35:1997–2008.

31. Yan CG, Craddock RC, He Y, Milham MP. Addressing head motion dependencies for small-world topologies in functional connectomics. Front Hum Neurosci 2013;7:910.

32. Seeley WW, Menon V, Schatzberg AF, et al. Dissociable intrinsic connectivity networks for salience processing and executive control. J Neurosci 2007;27:2349–2356.

33. Raichle ME, MacLeod AM, Snyder AZ, et al. A default mode of brain function. Proc Natl Acad Sci U S A 2001;98:676–682.

34. Fox MD, Snyder AZ, Vincent JL, et al. The human brain is intrinsically organized into dynamic, anticorrelated functional networks. Proc Natl Acad Sci U S A 2005;102:9673–9678.

35. Desikan RS, Segonne F, Fischl B, et al. An automated labeling system for subdividing the human cerebral cortex on MRI scans into gyral based regions of interest. Neuroimage 2006;31:968–980.

36. Fransson P. Spontaneous low-frequency BOLD signal fluctuations: an fMRI investigation of the resting-state default mode of brain function hypothesis. Hum Brain Mapp 2005;26:15–29.

37. Qin P, Di H, Liu Y, et al. Anterior cingulate activity and the self in disorders of consciousness. Hum Brain Mapp 2010;31:1993–2002.

38. Coleman MR, Rodd JM, Davis MH, et al. Do vegetative patients retain aspects of language comprehension? Evidence from fMRI. Brain 2007;130:2494–2507.

39. Andronache A, Rosazza C, Sattin D, et al. Impact of functional MRI data preprocessing pipeline on default-mode network detectability in patients with disorders of consciousness. Front Neuroinform 2013;7:16.

40. Crone JS, Soddu A, Holler Y, et al. Altered network properties of the fronto-parietal network and the thalamus in impaired consciousness. Neuroimage Clin 2013;4:240–248.

41. Rumsey DJ. Statistics for dummies. 2nd ed. Hoboken, NJ: Wiley, 2011.

42. Cordes D, Haughton V, Carew JD, et al. Hierarchical clustering to measure connectivity in fMRI resting-state data. Magn Reson Imaging 2002;20:305–317.

43. Youden WJ. Index for rating diagnostic tests. Cancer 1950;3:32–35.

44. Schrouff J, Perlbarg V, Boly M, et al. Brain functional integration decreases during propofol-induced loss of consciousness. Neuroimage 2011;57:198–205.

45. Crone JS, Holler Y, Bergmann J, et al. Self-related processing and deactivation of cortical midline regions in disorders of consciousness. Front Hum Neurosci 2013;7:504.

46. Medford N, Critchley HD. Conjoint activity of anterior insular and anterior cingulate cortex: awareness and response. Brain Struct Funct 2010;214:535–549.

47. Schiff ND. Recovery of consciousness after brain injury: a mesocircuit hypothesis. Trends Neurosci 2010;33:1–9.

48. Mukamel EA, Pirondini E, Babadi B, et al. A transition in brain state during propofol-induced unconsciousness. J Neurosci 2014; 34:839–845.

49. Langsjo JW, Alkire MT, Kaskinoro K, et al. Returning from oblivion: imaging the neural core of consciousness. J Neurosci 2012; 32:4935–4943.

50. Beissner F, Meissner K, Bar KJ, Napadow V. The autonomic brain: an activation likelihood estimation meta-analysis for central processing of autonomic function. J Neurosci 2013;33:10503–10511.

51. Qin P, Northoff G. How is our self related to midline regions and the default-mode network? Neuroimage 2011;57:1221–1233.

52. Mason MF, Norton MI, Van Horn JD, et al. Wandering minds: the default network and stimulus-independent thought. Science 2007; 315:393–395.

53. Schilbach L, Eickhoff SB, Rotarska-Jagiela A, et al. Minds at rest? Social cognition as the default mode of cognizing and its putative relationship to the "default system" of the brain. Conscious Cogn 2008;17:457–467.

54. Horovitz SG, Fukunaga M, de Zwart JA, et al. Low frequency BOLD fluctuations during resting wakefulness and light sleep: a simultaneous EEG-fMRI study. Hum Brain Mapp 2008;29:671–682.

55. Boly M, Phillips C, Tshibanda L, et al. Intrinsic brain activity in altered states of consciousness: how conscious is the default mode of brain function? Ann N Y Acad Sci 2008;1129:119–129.

56. Stender J, Kupers R, Rodell A, et al. Quantitative rates of brain glucose metabolism distinguish minimally conscious from vegetative state patients. J Cereb Blood Flow Metab 2015;35:58–65.